

## Optimization of Flow Rate for Improving Performance and Stability of Ni-YSZ based Solid Oxide Fuel Cells Using CH<sub>4</sub> Fuel

Jae-ha Myung<sup>1</sup>, Hyun Jun Ko<sup>1,2</sup>, Jong-Jin Lee<sup>1</sup> and Sang-Hoon Hyun<sup>1,\*</sup>

<sup>1</sup> School of Advanced Materials Science and Engineering, Yonsei University, Seoul 120-749, South Korea

<sup>2</sup> Specialized Graduate School of Hydrogen & Fuel Cell, Yonsei University, Seoul 120-749, South Korea

\*E-mail: [prohsh@yonsei.ac.kr](mailto:prohsh@yonsei.ac.kr)

Received: 19 March 2011 / Accepted: 14 April 2011 / Published: 1 May 2011

---

The advantages of solid oxide fuel cells (SOFCs), compared with other types of fuel cells, include their high energy conversion efficiency and their utilization of hydrocarbon fuels without reformers. Although conventional Ni-based cermet anodes have commonly been used as an anode material with high catalytic properties for H<sub>2</sub> fuel, the carbon deposition in Ni-YSZ anodes when hydrocarbon fuels are used directly is a critical problem that results in the destruction of the anode microstructure and abrupt decline in cell performance. Our research focuses on optimizing the flow rate of CH<sub>4</sub>-fueled Ni-YSZ anode/YSZ electrolyte/LSM-YSZ cathode type SOFC unit cells for improving cell performance and better durability. A high power density of 0.75 Wcm<sup>-2</sup> at 800 °C, 0.5 Wcm<sup>-2</sup> at 700 °C and 0.4 Wcm<sup>-2</sup> at 650 °C using CH<sub>4</sub> fuel as well as excellent durability were obtained via optimization of CH<sub>4</sub> flow rate at 800 °C, 700 °C, and 650 °C operating temperatures. The different types of carbon that cause an increase or decrease in cell performance under certain operating conditions was also investigated.

---

**Keywords:** Solid oxide fuel cell, Ni-based anode supported unit cell, durability test, CH<sub>4</sub>.

### 1. INTRODUCTION

Solid oxide fuel cells (SOFCs) with low emission and high energy conversion efficiency can use hydrocarbon fuels directly without the use of a reformer, making them a very attractive energy device [1]. For hydrocarbon fuels, conventional Ni-based cermet anodes have commonly been used as an anode material because of their catalytic properties. However, carbon deposition is a critical problem that causes loss of cell performance and poor stability during internal reforming reactions [2-6]. Changing the composition of the fuel, the operating temperature, the catalyst support, the Ni

particle size, and the addition of various catalysts to prevent carbon formation all affect the rate of carbon deposition. Moreover, carbon has diverse structures including adsorbed polymeric, vermicular filaments, carbide, and graphitic, which affect carbon reactivity and result in degradation in catalytic activation [7-8]. Several studies of the characteristics of carbon deposited on Ni-YSZ have been sought to overcome carbon deposition. Alzate-Restrepo et al. [9] found that when current density was increased, less carbon was deposited and that, with increased operating time and anode thickness, deposited carbon became more difficult to remove. Lin, Zhan et al. [10] found that Ni-YSZ anode-supported SOFCs can be operated stably with high applied current density. It is also well known that carbon deposition is suppressed at high S/C ratios, lower operating temperatures, and when new anode catalysts such as ceria, ceramic anode and Alkali metals are used [11-19]. The utilization of carbon as a fuel for solid oxide fuel cells was further investigated by Ihara et al [20]. The CO<sub>2</sub> generated by the electrochemical oxidation of carbon reacted with the deposited carbon and produced CO. In turn, this CO can be used as fuel.

In this study, we fabricated Ni-YSZ anode-supported unit cells with a thin YSZ electrolyte using the dip-coating method and examined their maximum power density and durability at various CH<sub>4</sub> flow rates at temperatures between 650 °C and 800 °C. The results suggest that some useful small ball carbon may be deposited on the anode and the rate of carbon deposition can be minimized for improved cell performance by optimizing CH<sub>4</sub> flow rates at a given operating temperature.

## 2. EXPERIMENTAL

### 2. 1. Fabrication of unit cells

Conventional Ni-YSZ anode-supported unit cells were fabricated by uni-axial pressing, dip-coating and screen printing methods. The anode raw materials were NiO (Nickelous Oxide Green, J.T. Baker, USA), coarse YSZ (FYT13.0-010H, Unitec Ceramics, UK), fine YSZ (TZ-8Y, Tosoh, Japan), and carbon black (Raven 430, Columbian Chemical, USA) as pore former. The anode was produced with a mixture of 58.4 wt% NiO, 15.8 wt% coarse YSZ, 15.8 wt% fine YSZ and 10 wt% carbon black by uni-axial pressing method. The pre-sintered anode supports manufactured at 1200 °C were then dipped into fine YSZ slurry to coat them with a thin electrolyte layer. A thinner electrolyte reduces the ohmic resistance associated with the oxygen transport across the electrolyte and minimizes carbon formation on the anode side through a maximal carbon oxidation reaction. The thickness (6-10 μm) of YSZ electrolyte was controlled by withdrawal speeds during the dip-coating process, followed by sintering at 1350 °C to obtain a dense YSZ electrolyte. A cathode having a composition of 50 wt% LSM and 50 wt% fine YSZ was screen-printed to obtain 1 cm<sup>2</sup> active area on one side of the anode support electrolyte, while the other side was polished to remove the electrolyte coating. Finally, it was sintered at 1150 °C.

### 2. 2. Cell performance tests

In tests, unit cell performance was measured with apparatuses designed and built by our laboratory; this is described in detail in our previous study [21].

The performance of the Ni-YSZ anode supported unit cells that has 1 cm<sup>2</sup> active area was evaluated at various temperatures (650-800 °C) in reactive gases of H<sub>2</sub> (200 ccmin<sup>-1</sup> in standard ambient temperature and pressure) with either 3 % H<sub>2</sub>O or CH<sub>4</sub> (20-75 ccmin<sup>-1</sup> in standard ambient temperature and pressure) with 3 % H<sub>2</sub>O at the anode and air (500 ccmin<sup>-1</sup> in standard ambient temperature and pressure) at the cathode. The I-V characterization and durability were measured with a multi-functional electronic load module (3315D, Taiwan). AC impedance measurements were conducted with a Solatron 1260 frequency analyzer and a Solatron 1287 interface.

### 2. 3. Characteristics of deposited carbon

The microstructures of Ni-YSZ anode were observed with a scanning electronic microscope (SEM: Model S4200, Hitachi, Ltd., Japan) to compare the different forms of carbon deposited. The different forms of carbon on the anode were further examined by using temperature-programmed oxidation (TPO: Telcat-M). TPO was measured with a ramping temperature rate of 5 °Cmin<sup>-1</sup> and gas flow rate of 30 ccmin<sup>-1</sup> (20 % O<sub>2</sub> and 80 % He).

Carbon that leads to degradation of cell performance and to cracking of the anode microstructure was revealed to be a form of fiber, graphite, or amorphous carbon that is oxidized at 400~700 °C. In contrast, small ball carbon, which can enhance electrical conductivity in metallic phases and greatly improve power density, is oxidized at over 700 °C.

However, if the rate of carbon deposition is not controlled, the small ball carbon can transform into “flower-like” or poly-aromatic carbon through agglomeration [22-24]. Therefore, the optimal operating conditions for using CH<sub>4</sub> can be found by distinguishing between these two classes of deposited carbon.

## 3. RESULTS AND DISCUSSION

### 3.1. Evaluation of initial cell performance using H<sub>2</sub> and CH<sub>4</sub>

The unit cells were successfully fabricated with a thin electrolyte to obtain high power density by uni-axial pressing and dip-coating methods as shown in the SEM image in figure 1. The unit cell with 10 μm-thick YSZ electrolyte showed a maximum power density of 0.4 Wcm<sup>-2</sup> with H<sub>2</sub> at 800 °C.

However, the unit cell fabricated with 6 μm-thick YSZ electrolyte showed a 50 % improvement in maximum power density of 0.6 Wcm<sup>-2</sup>, and showed maximum power density of 0.75 Wcm<sup>-2</sup> for 30 ccmin<sup>-1</sup> of CH<sub>4</sub> fuel as shown in figure 2.

Even though the CH<sub>4</sub> flow rate increased to 75 ccmin<sup>-1</sup>, the cell performance deteriorated as illustrated in figure 3. As a result, the 30 ccmin<sup>-1</sup> CH<sub>4</sub> flow rate was chosen for the durability test.

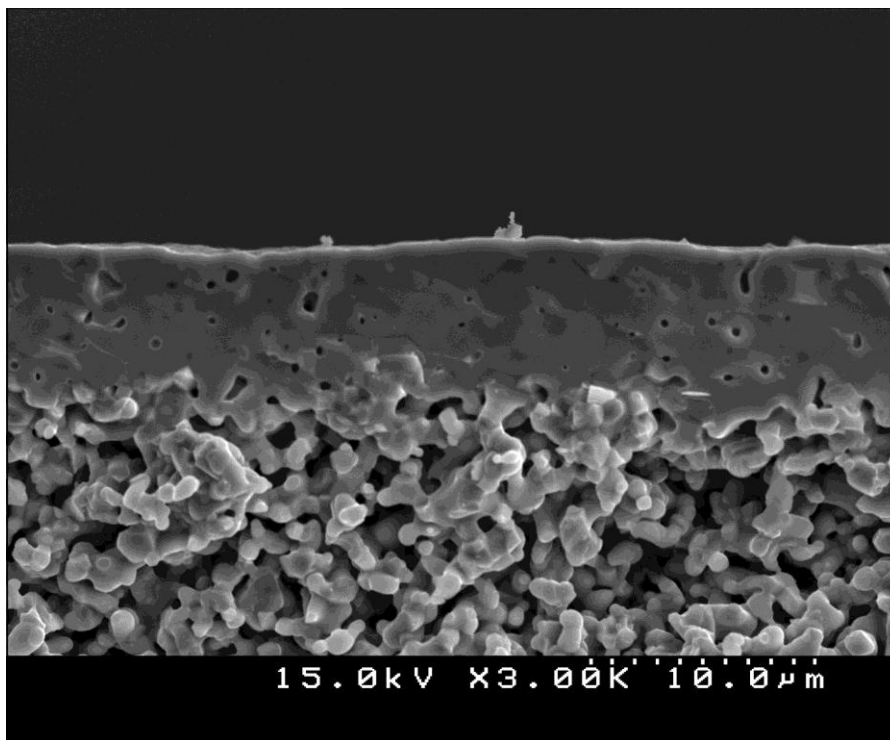


**Figure 1.** SEM image of a cross-sectional area of anode supported electrolyte fabricated by uni-axial pressing and dip-coating methods.

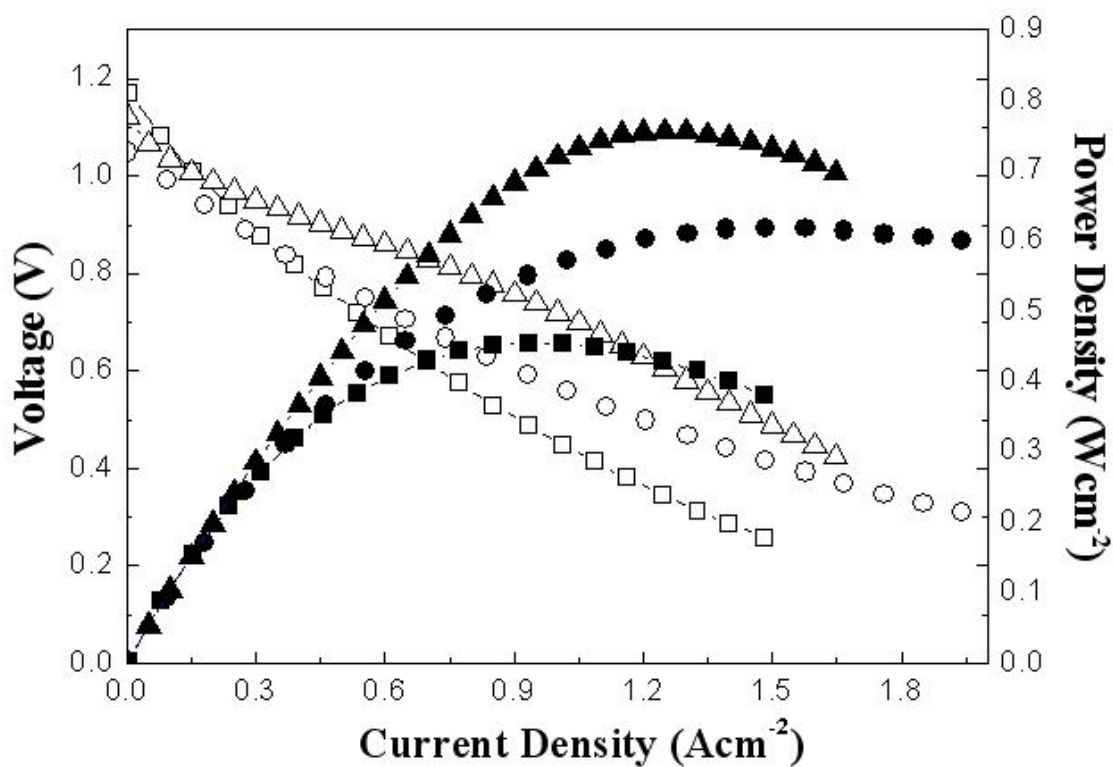


**Figure 2.** The I-V characteristics of the unit cell with 10 µm thickness of YSZ electrolyte ( ■ ), the unit cell with 6 µm thickness of YSZ electrolyte using humidified H<sub>2</sub> (200 ccmin<sup>-1</sup>) with 3% H<sub>2</sub>O and air (500 ccmin<sup>-1</sup>) ( ● ), and using CH<sub>4</sub> (30 ccmin<sup>-1</sup>) with 3% H<sub>2</sub>O ( ▲ ).

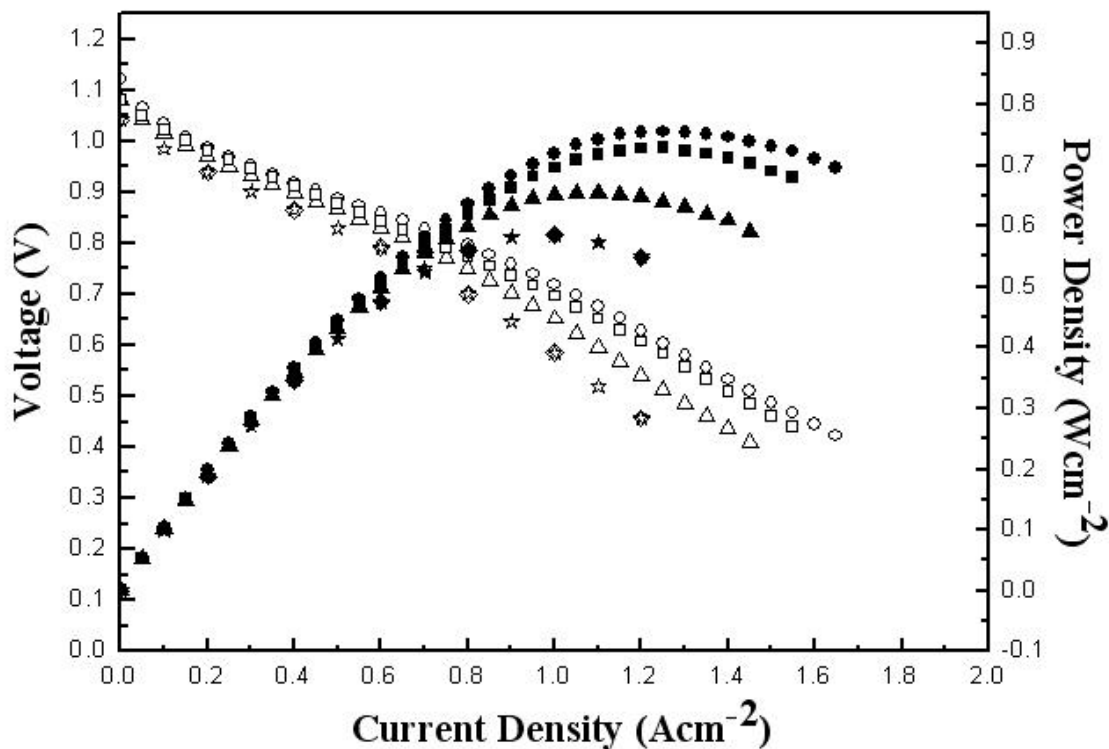


**Figure 3.** The I-V characteristics of the unit cell with various  $\text{CH}_4$  flow rates, 25 ( $\blacksquare$ ), 30 ( $\bullet$ ), 35 ( $\blacktriangle$ ), 55 ( $\blacklozenge$ ), 75 ( $\blackstar$ ) with 3%  $\text{H}_2\text{O}$  at 800 °C.

### 3.2. Conditions when fuels are changed ( $\text{H}_2 \rightarrow \text{CH}_4$ )

To operate Ni-YSZ based SOFCs using  $\text{CH}_4$  with minimal cell degradation, they must be operated under polarization conditions to reduce carbon deposition [25-26]. As well,  $\text{CH}_4$  concentrations must be gradually increased in order to not affect stability. Moreover, a thinner electrolyte is a major factor to attain higher current densities and reduce carbon formation rates by increasing oxygen transport. The case of a conventional Ni-YSZ unit cell with a 10  $\mu\text{m}$ -thick electrolyte is supplied with 50  $\text{ccmin}^{-1}$  of  $\text{CH}_4$  flow rate showed rapid degradation in cell performance. However, the stability of a unit cell supplied with an optimized  $\text{CH}_4$  flow rate (30  $\text{ccmin}^{-1}$ ) was improved despite lower voltage. On the other hand, a unit cell with a 6  $\mu\text{m}$  minimized thickness of electrolyte at a 30  $\text{ccmin}^{-1}$   $\text{CH}_4$  flow rate showed highest initial voltage and better durability as shown in figure 4.

After stabilization, the unit cells with 6  $\mu\text{m}$  minimized thickness of electrolyte at a 30  $\text{ccmin}^{-1}$   $\text{CH}_4$  flow rate showed much smaller ohmic resistance and anodic polarization resistance than did those using  $\text{H}_2$ , as shown in figure 5. Usually, anodic polarization resistance using  $\text{CH}_4$  fuel is higher than that using  $\text{H}_2$ , because of the higher mass of  $\text{CH}_4$  molecules, slower electrochemical oxidation and deposited carbon [13, 27]. However, in this case, if the amount of  $\text{CH}_4$  supplied is optimized under applied current, the anodic polarization resistance can be reduced through increased electrical conductivity and the carbon oxidation reaction by oxygen ion transfer. As well, the rate of carbon

removal as well as the amount of carbon formed during the gas phase reaction is optimized and the resulting minimized carbon deposits enhance electrical conductivity [28].

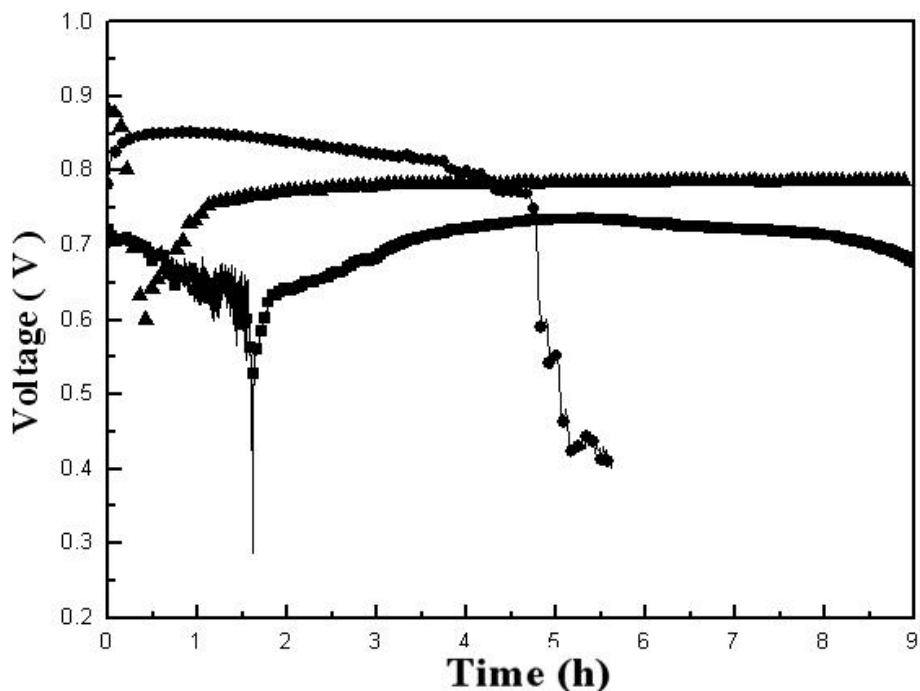


**Figure 4.** Long-term stability test of the unit cell with 10  $\mu\text{m}$  thickness of YSZ electrolyte ( ■ ), the unit cell with 6  $\mu\text{m}$  thickness of YSZ electrolyte ( ▲ ) using  $\text{CH}_4$  ( $30 \text{ ccmin}^{-1}$ ) with 3%  $\text{H}_2\text{O}$ , and the unit cell with 10  $\mu\text{m}$  thickness of YSZ electrolyte using  $\text{CH}_4$  ( $50 \text{ ccmin}^{-1}$ ) with 3%  $\text{H}_2\text{O}$  ( ● ).

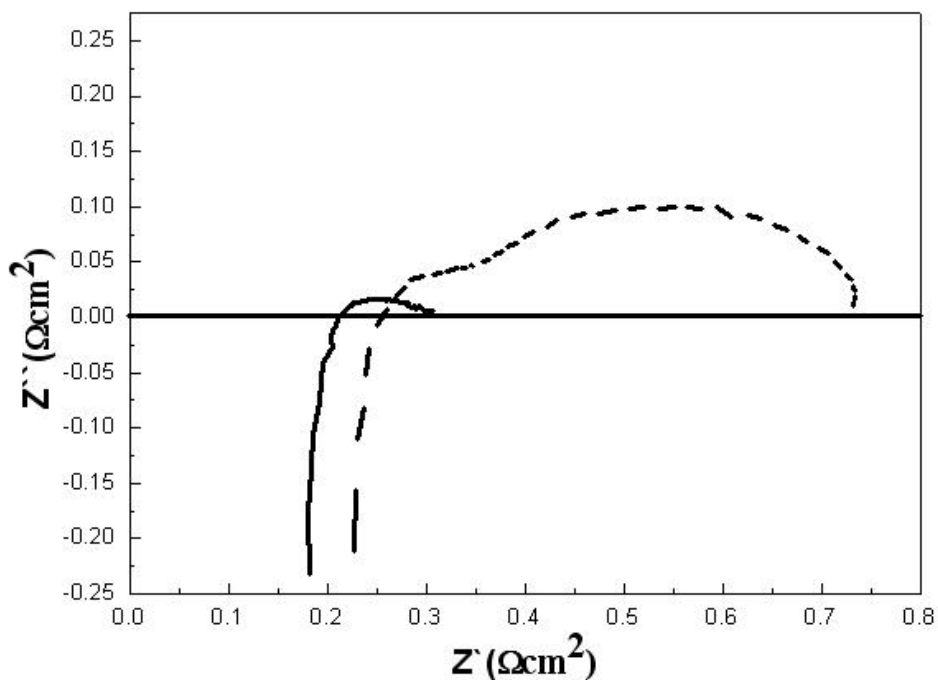


**Figure 5.** Impedance spectra for the unit cell using  $\text{H}_2$  (---) and  $\text{CH}_4$  (—).

3.3. Evaluation of cell performance at various operating temperatures and CH<sub>4</sub> flow rates

The maximum power density for 30 ccmin<sup>-1</sup> of CH<sub>4</sub> with applied 0.4 current density at 800 °C is 0.71 Wcm<sup>-2</sup> for 54 hours of operation without degradation in performance.

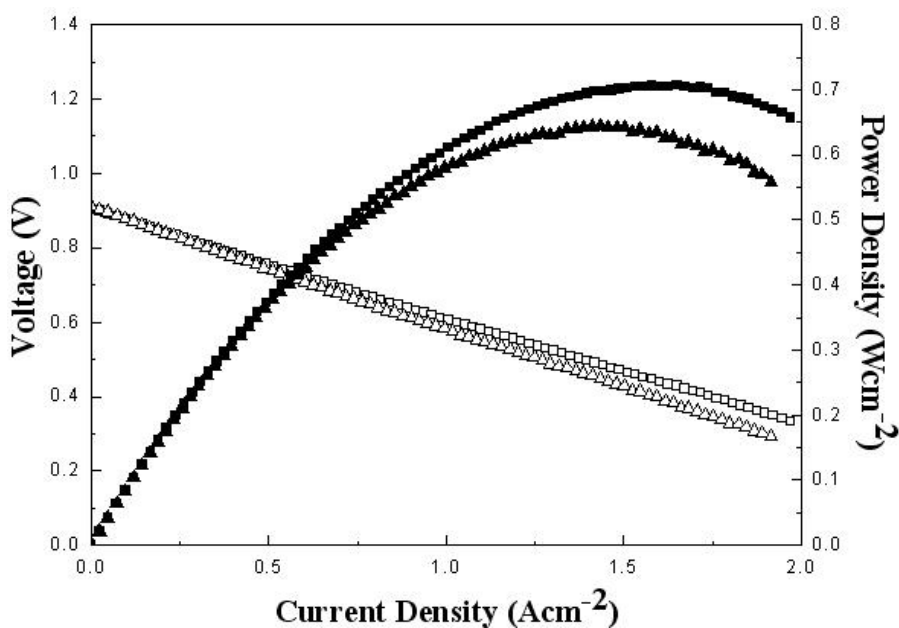


**Figure 6.** The I-V characteristics of the unit cell using 30 ccmin<sup>-1</sup> CH<sub>4</sub> flow rates ( ■ ), 25 ccmin<sup>-1</sup> CH<sub>4</sub> flow rate after 96 hours of total operation ( ▲ ) with 3% H<sub>2</sub>O at 800 °C.

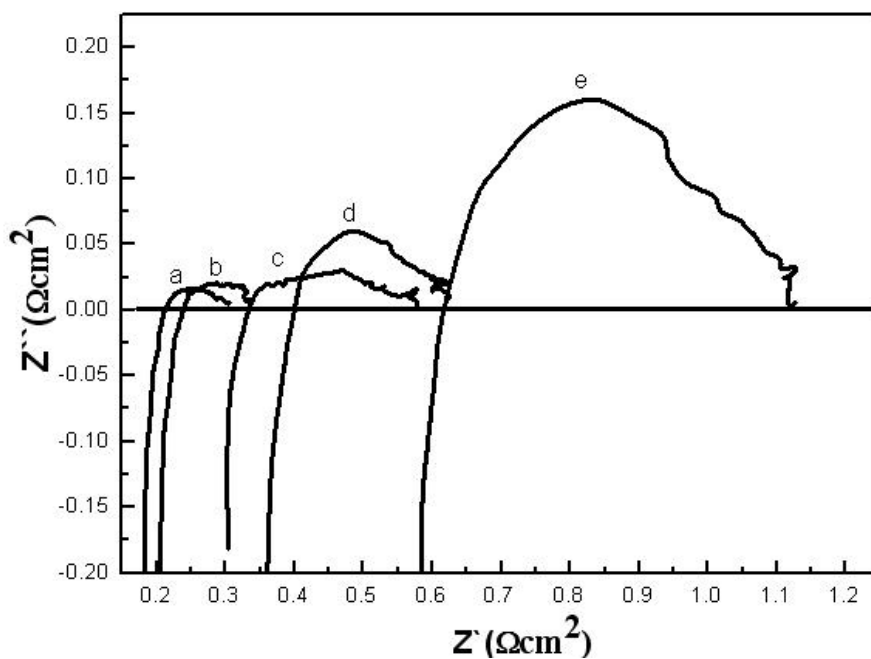


**Figure 7.** Impedance spectra for initial ( a ), after 54 hours for 30 ccmin<sup>-1</sup> CH<sub>4</sub> flow rates ( b ), and initial ( c ), after 15 hours ( d ), after 27 hours ( e ) for 25ccmin<sup>-1</sup> CH<sub>4</sub> flow rates with 3% H<sub>2</sub>O at 800 °C.

However, a 25 ccmin<sup>-1</sup> CH<sub>4</sub> flow rate showed 0.65 Wcm<sup>-2</sup> of maximum power density and degradation in performance as carbon deposition increased in figure 6. Looking at the impedance spectra data in figure 7, a CH<sub>4</sub> flow rate of 30 ccmin<sup>-1</sup> showed similar ohmic resistance and anodic polarization resistance for 54 hours of operation.

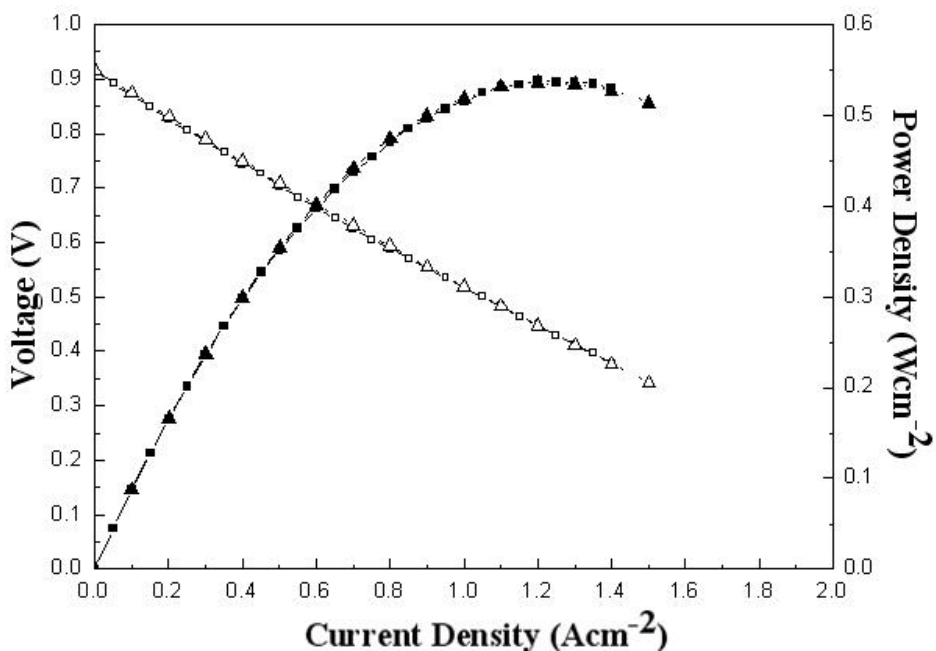


**Figure 8.** The I-V characteristics of initial ( ■ ) and after 120 hours of operation (total operation, 200 hours) ( ▲ ) for 25 ccmin<sup>-1</sup> CH<sub>4</sub> flow rates with 3% H<sub>2</sub>O at 700 °C.

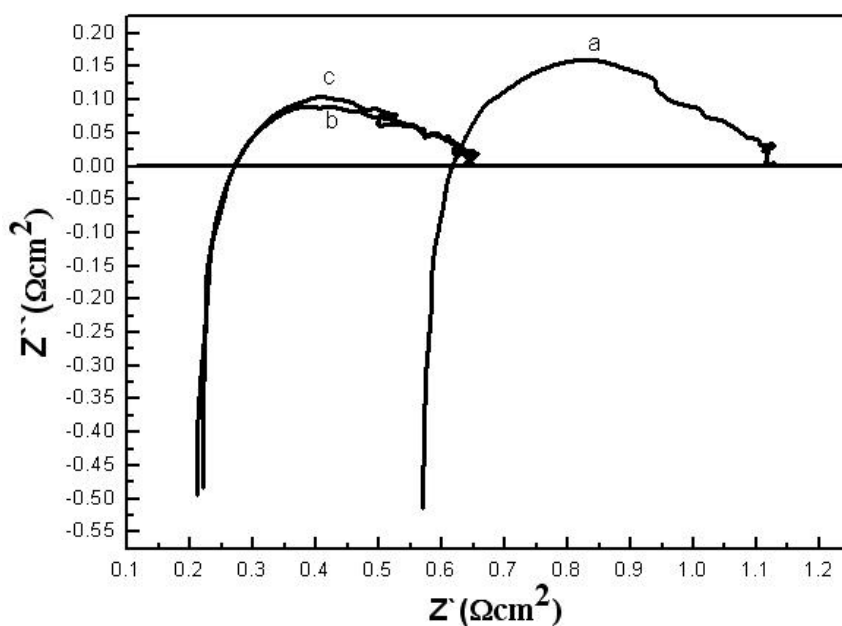


**Figure 9.** Impedance spectra after 96 hours of total operation for 25 ccmin<sup>-1</sup> CH<sub>4</sub> flow rates at 800 °C ( a ), and initial ( b ) and after 120 hours ( c ) of operation for 25 ccmin<sup>-1</sup> CH<sub>4</sub> flow rates with 3% H<sub>2</sub>O at 700 °C.



However, ohmic resistance and anodic polarization resistance gradually increased in the case of  $25 \text{ ccmin}^{-1}$  of  $\text{CH}_4$  at  $800 \text{ }^\circ\text{C}$ . This is because both the rate of carbon removal through electrochemical reaction and the rate of carbon formation during the gas phase reaction are equilibrated and optimal by  $30 \text{ ccmin}^{-1}$  flow rate at  $800 \text{ }^\circ\text{C}$ .

We then lowered the operating temperature to  $700 \text{ }^\circ\text{C}$  and then again to  $650 \text{ }^\circ\text{C}$ . The ohmic resistance reduced from  $0.58 \text{ } \Omega\text{cm}^{-2}$  at  $800 \text{ }^\circ\text{C}$  to  $0.25 \text{ } \Omega\text{cm}^{-2}$  at  $700 \text{ }^\circ\text{C}$  despite the decrease in operating temperatures, because the equilibrated condition is reset by  $25 \text{ ccmin}^{-1}$  flow rate at  $700 \text{ }^\circ\text{C}$ . As well, after the cell operated for 120 hours at  $700 \text{ }^\circ\text{C}$  with  $25 \text{ ccmin}^{-1}$  of  $\text{CH}_4$ , no degradation in cell performance was observed in the I-V curve and impedance spectra as shown in figures 8 and 9.

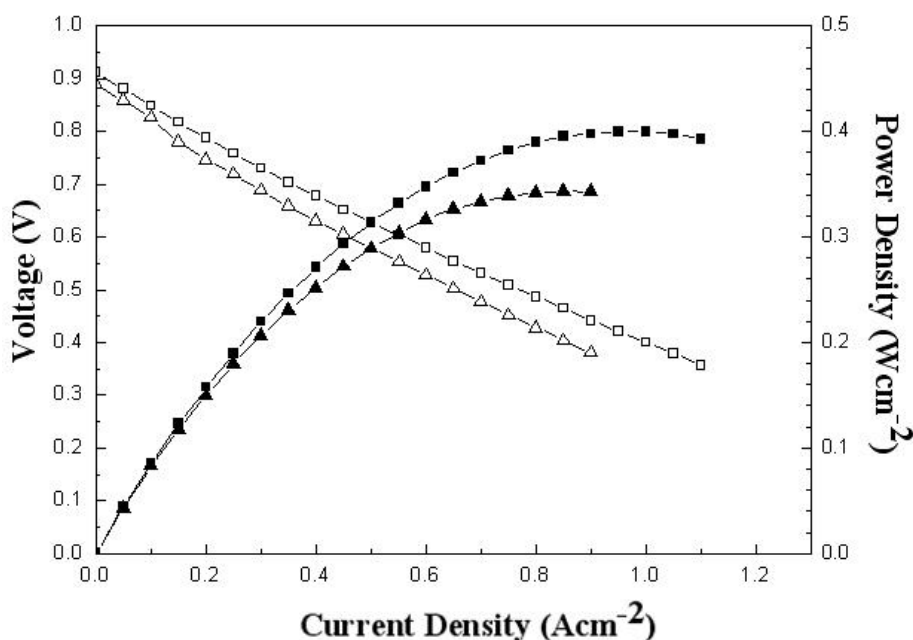


**Figure 10.** The I-V characteristics of the unit cell using  $25 \text{ ccmin}^{-1}$   $\text{CH}_4$  flow rates at initial ( ■ ) and after 170 hours of operation (total operation, 370 hours) ( ▲ ) with 3%  $\text{H}_2\text{O}$  at  $650 \text{ }^\circ\text{C}$ .

However, in the I-V curve and impedance spectra at  $650 \text{ }^\circ\text{C}$  of figures 10 and 11, cell power density slowly decreased to  $0.35 \text{ Wcm}^{-2}$  after 170 hours. Figure 12 summarizes the long-term stability results obtained for conventional Ni-YSZ based SOFCs using  $\text{CH}_4$  at various temperatures and with different  $\text{CH}_4$  flow rates. At  $800 \text{ }^\circ\text{C}$ ,  $30 \text{ ccmin}^{-1}$  of  $\text{CH}_4$  was more stable than  $25 \text{ ccmin}^{-1}$ , but the cell is re-stabilized when the operating temperature was lowered and  $\text{CH}_4$  was supplied at  $25 \text{ ccmin}^{-1}$ . Then, cell performance at  $650 \text{ }^\circ\text{C}$  degraded gradually for 170 hours due to carbon deposition. From the results, it is found that the stability of  $\text{CH}_4$ -fueled SOFC is relative with the rate of carbon removal and it of carbon formation. If the removal rate is faster than the formative rate, it leads to oxidize the deposited carbon has electrical conductivity. In the other case, the formative rate is faster than the removal rate, which accelerates to deposit carbon that blocks the anode pore and crack the anode micro-structure.

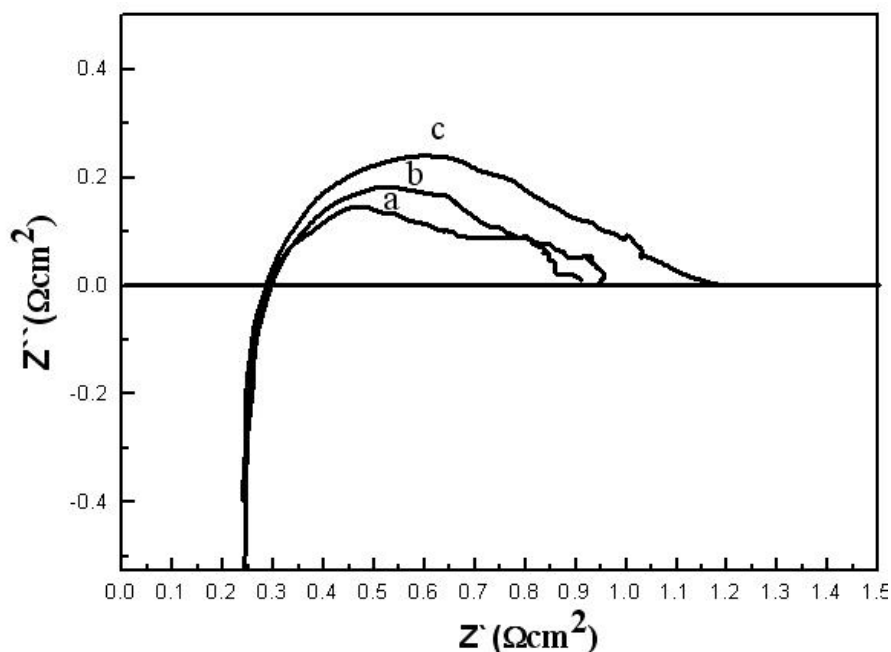


**Figure 11.** Impedance spectra for initial ( a ), after 27 hours ( b ), after 170 hours ( c ) for 25 ccmin<sup>-1</sup> CH<sub>4</sub> flow rates with 3% H<sub>2</sub>O at 650 °C.

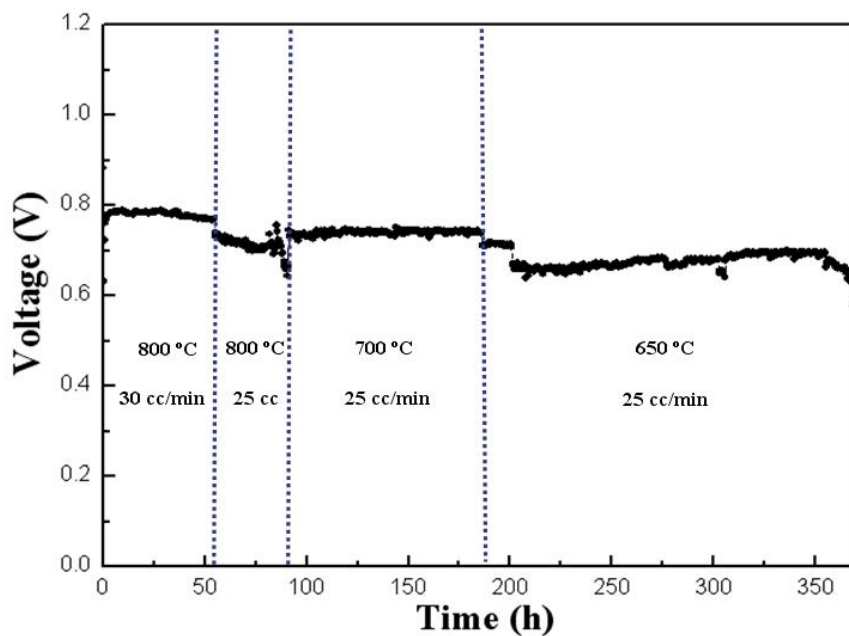


**Figure 12.** Summarized result of long-term stability test for various temperatures and CH<sub>4</sub> flow rate with 0.4 applied current density.

### 3. 4. Anode analysis after CH<sub>4</sub> fueled operation

The characteristics of the carbon deposited on the anode surface were investigated by analyzing the conventional Ni-YSZ both under and in the absence of optimized operating conditions. The SEM

images in figure 13 show the different types of carbon that were formed on in the anode near electrochemically active region.

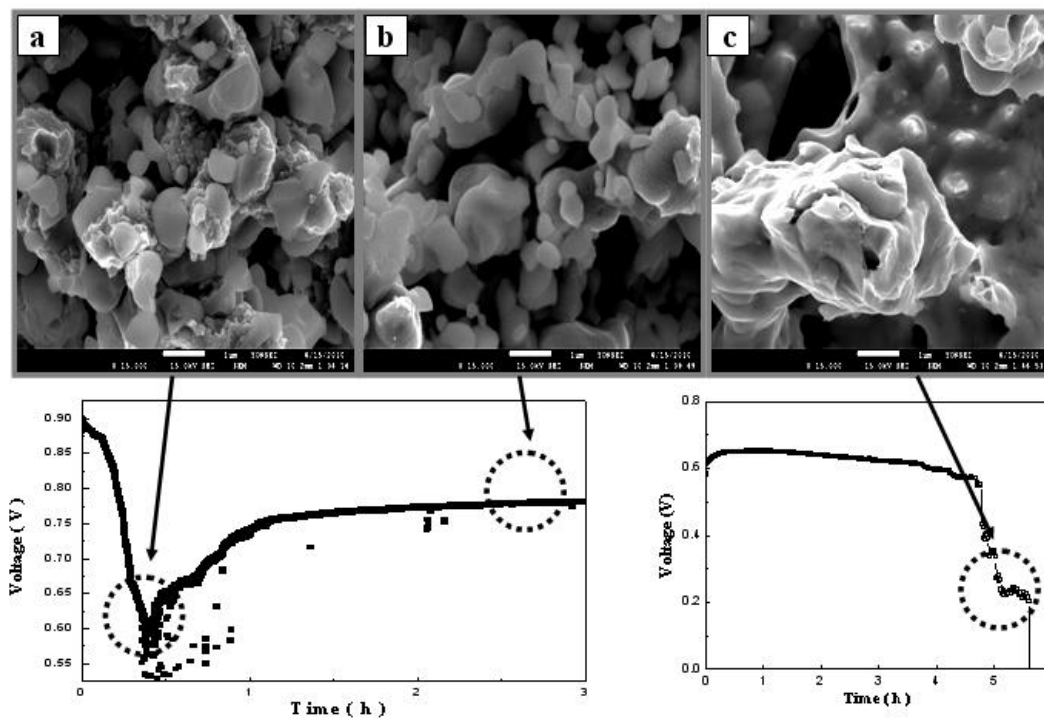


**Figure 13.** SEM images of the anode section with 30 ccmin<sup>-1</sup> CH<sub>4</sub> flow rate at initial degradation ( a ) and under stable operation ( b ) and the anode section with 75 ccmin<sup>-1</sup> after operation stop ( c ).

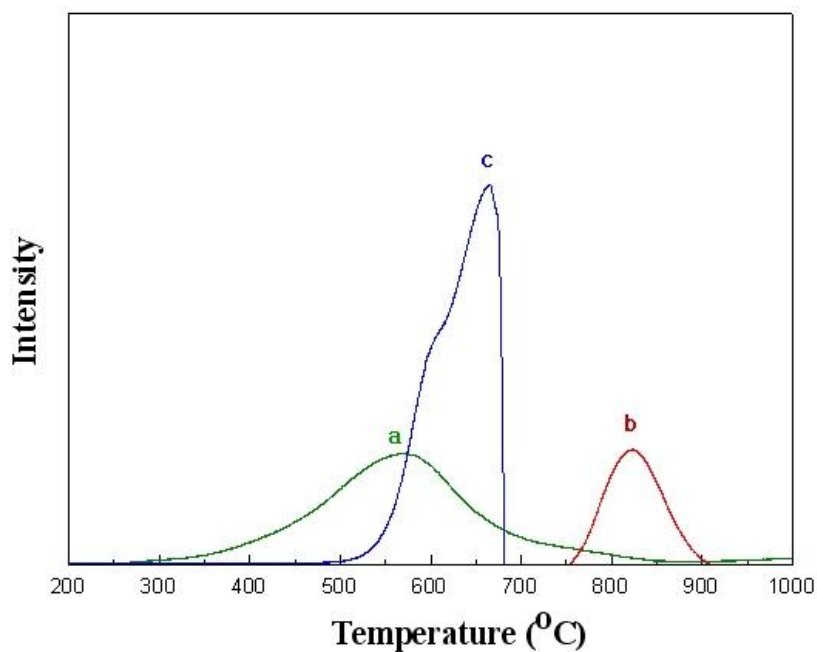


**Figure 14.** Temperature-programmed oxidation results for the anode at initial degradation ( a ), under stable operation ( b ) and after operation stop ( c ).

The graphite carbon causes cell expansion and provokes a crash in the microstructure of the anode, which is oxidized at around 700 °C. In the case of Ni-YSZ unit cells operated outside of particular operating conditions which are not with optimal CH<sub>4</sub> flow rate and under polarization conditions, graphite carbon was deposited on the anode as the SEM image as figure 13c illustrates. Figure 13a shows that fiber or amorphous carbon that is usually oxidized under 600 °C was deposited during initial degradation.

During stable operation, small ball carbon that enhances power density and electrical conductivity is deposited on the anode. Furthermore, small ball carbon did not accumulate and form the poly-aromatic carbons that block the microstructures of anodes during the period of optimized testing as figure 13b illustrates. As shown in figure 14, it is confirmed that the fiber or amorphous carbon at initial degradation is changed to small ball carbon after stabilizing condition. If excessive CH<sub>4</sub> supplied in the unit cell, the fiber, amorphous carbon, and graphite are deposited in the anode. The quantities of these carbons are much larger than it of small ball carbon that is deposited at stable condition. The TPO, SEM and voltage graph results illustrate that cell stability and power density gradually improved under optimized CH<sub>4</sub> flow rate through the transformation of amorphous carbon into small ball carbon without increasing in the amount of carbon

#### 4. CONCLUSION

Thin YSZ electrolytes (6 μm thick) can be successfully fabricated on Ni-YSZ anode supports to obtain higher oxygen ionic conductivity by dip-coating them in YSZ slurry. These conventional Ni-YSZ unit cells showed much lower ohmic and anodic polarization resistance and higher performance and improved stability by controlling CH<sub>4</sub> flow rates. It was confirmed that the optimal CH<sub>4</sub> flow rates for operating CH<sub>4</sub>-fueled cells are 30 ccmin<sup>-1</sup> at 800 °C, 25 ccmin<sup>-1</sup> at 700 °C, and 20 ccmin<sup>-1</sup> at 650 °C by controlling the amount and the type of carbon deposited under given operating conditions. The CH<sub>4</sub> fueled unit cell showed maximum power densities of 0.75, 0.53, and 0.4 Wcm<sup>-2</sup> at 800 °C, 700 °C, and 650 °C, respectively, in CH<sub>4</sub> humidified with 3 % H<sub>2</sub>O and operated for over 370 hours without serious degradation.

#### ACKNOWLEDGEMENTS

This work was supported by the Seoul R&BD Program (CS070157).

#### References

1. S.A. Barnett In: W. Vielstich, A. Lamm, H. Gasteiger, Editors, Handbook of Fuel Cell Technology IV, *Fundamentals of Technology and Applications*, p. 1098, Wiley, San Francisco (2003).
2. J. Mermelstein, M. Millan, N.P. Brandon, *Chem Eng Sci* ., 64, (2009) 492.
3. M. Ni, D.Y.C. Leung, M.K.H. Leung, K. Sumathy, *Fuel Processing Technol.*, 87, (2006) 461.
4. P. McKendry, *Bioresource Technol* ., 83, (2002) 55.
5. Y. Cao, Y. Wang, J.T. Riley, W.-P. Pan, *Fuel Processing Technol.*, 87, (2006) 343.

6. A.L. Dicks, *J. Power Sources.*, 61, (1982) 113.
7. C.H. Bartholomew, *Catal. Rev. -Sci. Eng.*, 24, (1982) 67.
8. P.G. Menon, *J. Mol. Catal.*, 59, (1990) 207.
9. Alzate-Restrepo, J. M. Hill, *Appl Catal A Gen.*, 342, (2008) 49.
10. Y. Lin, Z. Zhan, J. Liu, S.A. Barnett, *Solid State Ion.*, 176, (2005) 1827.
11. T. Hibino, A. Hashimoto, T. Inoue, J.-I. Tokuno, S.-I. Yoshida, M. Sano, *Science*, 288, (2000) 2031.
12. B.C.H. Steele, *Solid State Ion.*, 86, (1996) 1223.
13. E.P. Murray, T. Tsai, S.A. Barnett, *Nature*, 400, (1999) 649.
14. S. Park, J.M. Vohs, R.J. Gorte, *Nature*, 404, (2000) 265.
15. R.H. Cunningham, C.M. Finnerty, R.M. Ormerod In: U. Stimming, S.C. Singhal, H. Tagawa, W. Lehnert, Editors, Proceedings of Fifth International Symposium on Solid Oxide Fuel Cells, p. 973, *The Electrochemical Society Proceedings Series*, Pennington, NJ (1997).
16. H. Praliaud, M. Primet, G.A. Martin. *Appl. Surf. Sci.*, 17, (1983) 107.
17. H. Praliaud, J.A. Dalmon, C. Mirodatos, G.A. Martin. *J. Catal.*, 97, (1986) 344.
18. J.R. Rostrup-Nielsen, L.J. Christiansen. *Appl. Catal. A: General.*, 126, (1995) 381.
19. J. H. Myung, J. J. Lee, S. H. Hyun, *Electrochem. Solid-State Lett.*, 13, (2010) B43.
20. S. Hasegawa, M. Ihara, *J. Electrochem. Soc.*, 155, (2008) B58.
21. S.D. Kim, H. Moon, S.H. Hyun, J. Moon, J. Kim, H.W. Lee, *Solid State Ion.*, 177, (2006) 931.
22. H. He, J.M. Vohs, R. J. Gorte, *J. Power Sources.*, 144, (2005)135.
23. J. Mermelstein, M. Millan, N. P. Brandon, *Chem. Eng. Sci.*, 64, (2009) 492.
24. C. M. Finnerty, N. J. Coe, R. H. Cunningham, R. M. Ormerod, *Catal. Today.*, 46, (1998) 137.
25. M. Pillai, Y. Lin, H. Zhu, R. J. Kee, S. A. Barnett, *J. Power Sources.*, 195, (2010) 271 .
26. Y. Lin, Z. Zhan, J. Liu and S.A. Barnett, *Solid State Ion.*, 176, (2005)1827.
27. J. Liu, S. A. Barnett, *Solid State Ion.*, 158, (2003)11.
28. H. Kim, C. Lu, W. L. Worrell, J. M. Vohs, R. J. Gorte, *J. Electrochem. Soc.*, 149, (2002) A247.